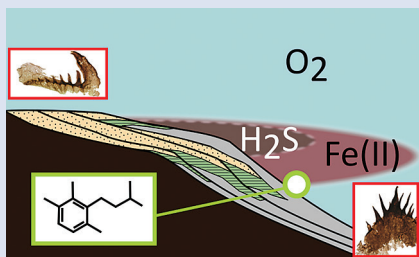# Oxygen minimum zones in the early Cambrian ocean

R. Guilbaud[1,2*], B.J. Slater[2,3], S.W. Poulton[4], T.H.P. Harvey[5],
J.J. Brocks[6], B.J. Nettersheim[6,7], N.J. Butterfield[2]

OPEN ACCESS

Abstract

The relationship between the evolution of early animal communities and oceanic oxygen levels remains unclear. In particular, uncertainty persists in reconstructions of redox conditions during the pivotal early Cambrian (541-510 million years ago, Ma), where conflicting datasets from deeper marine settings suggest either ocean anoxia or fully oxygenated conditions. By coupling geochemical palaeo-redox proxies with a record of organic-walled fossils from exceptionally well-defined successions of the early Cambrian Baltic Basin, we provide evidence for the early establishment of modern-type oxygen minimum zones (OMZs). Both inner- and outer-shelf environments were pervasively oxygenated, whereas mid-depth settings were characterised by spatially oscillating anoxia. As such, conflicting redox signatures recovered from individual sites most likely derive from sampling bias, whereby anoxic conditions represent mid-shelf environments with higher productivity. This picture of a spatially restricted anoxic wedge contrasts with prevailing models of globally stratified oceans, offering a more nuanced and realistic account of the Proterozoic-Phanerozoic ocean transition.

Introduction

The dramatically increased diversity of metazoan life through the late Ediacaran to early Cambrian transition (~585-510 Ma) coincides with a protracted transition from global ocean anoxia to widespread ocean oxygenation (Canfield *et al.*, 2007; Chen *et al.*, 2015; Von Strandmann *et al.*, 2015; Li *et al.*, 2017). Throughout the Proterozoic Eon (2500 to 541 Ma), the ocean is thought to have been characterised by oxygenated surface waters overlying euxinic (anoxic and sulphidic) mid-depth waters along productive ocean margins (Poulton *et al.*, 2010), and ferruginous (anoxic, Fe-containing) deeper waters (Planavsky *et al.*, 2011; Poulton and Canfield, 2011). Models for later Neoproterozoic oceans (635 to 541 Ma) also envisage redox stratification, with oscillations from strict anoxia to fully oxic conditions (Canfield *et al.*, 2007, 2008; Wood *et al.*, 2015). This dynamic ocean stratification is assumed to have persisted until the mid-Cambrian (Gill *et al.*, 2011; Chen *et al.*, 2015), by which time many key metazoan innovations had evolved.

Animals are fundamentally aerobic organisms - albeit with hugely varying oxygen demands - and their early fossil record is accordingly limited to oxygenated settings (Tostevin *et al.*, 2016). Most current models linking early animal evolution to redox chemistry assume a horizontally stratified ocean (Wood *et al.*, 2015; Jin *et al.*, 2016). However, modern oceans exhibit a marked lateral redox variability, most notably where combinations of high primary productivity and metazoan activity (Bianchi *et al.*, 2013) give rise to wedge-shaped oxygen minimum zones (Sperling *et al.*, 2015a). Determining which of these two models, horizontal or lateral, best characterises the structure of early Palaeozoic oceans is challenged by a dearth of spatial and temporal resolution, compounded by the removal of off-shelf signals due to subduction. Here, we exploit exceptionally well-preserved successions from the Baltic Basin to derive a high resolution redox model of early to middle Cambrian shelf seas (full details of geological setting and methods are provided as Supplementary Information).

Stratigraphy and Depositional Environments

We examined marine sediments from eight drill cores (Finngrundet-1, Bårstad-2, Bernstorp-1, Hamnudden-1, Böda Hamn-1, File Haidar-1, Grötlingbo-1 and Kostovo-13) spanning an area of 400 by 600 km across the Baltic Basin (Fig. 1). Studied sediments encompass the Lontova, File Haidar and Borgholm formations, deposited between the early Cambrian

1. Lancaster Environment Centre, Lancaster University, Lancaster LA1 4YQ, UK
2. Department of Earth Sciences, University of Cambridge, Cambridge CB2 3EQ, UK
*   Corresponding author (email: r.guilbaud@cantab.net)
3. Department of Earth Sciences, Paleobiology, Uppsala University, 75236 Uppsala, Sweden
4. School of Earth and Environment, University of Leeds, Leeds LS2 9JT, UK
5. Department of Geology, University of Leicester, Leicester LE1 7RH, UK
6. Research School of Earth Sciences, The Australian National University, ACT 2601, Australia
7. Max Planck Institute for Biogeochemistry, Hans-Knoell-Strasse 10, 07745 Jena, Germany
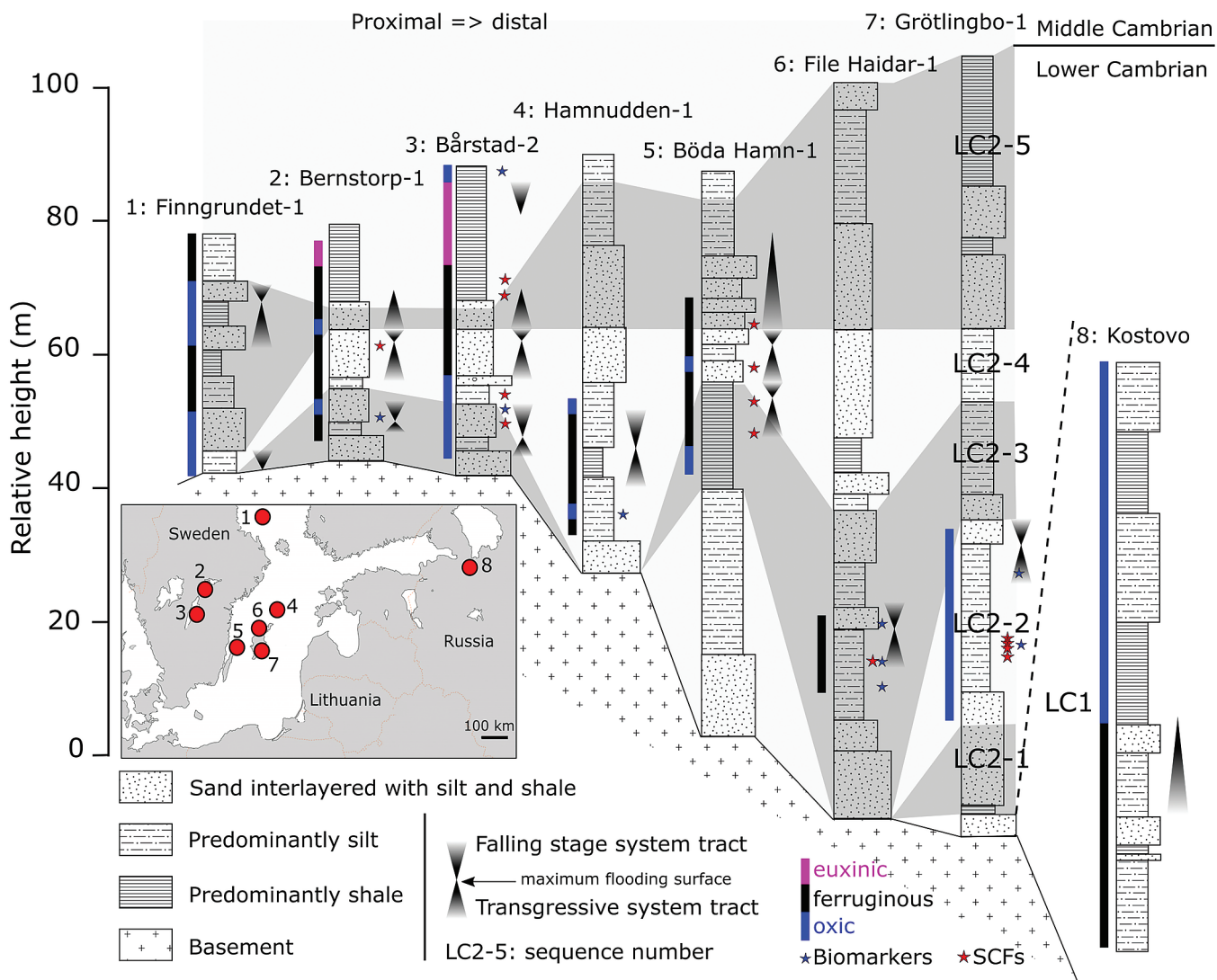
Figure 1 Core location (red circles) and stratigraphy, modified after Nielsen and Schovsbo (2011). Grey and white shadings represent the stratigraphic sequences (*e.g.*, LC2-5). The bars illustrate the analysed core sections (on mudstones and siltstones only); euxinic, ferruginous and oxic depositions are in purple, black and blue, respectively.

Fortunian stage and middle Cambrian Stage 5, and the internal stratigraphy and depositional environments of these siliciclastic sediments has been studied extensively (Hagenfeldt, 1994; Nielsen and Schovsbo, 2011, 2015). The studied area records a partial, yet substantial archive of contiguous sequences, organised into two supersequences for the lower Cambrian, 'LC1' and 'LC2', and one supersequence for the lower middle Cambrian, 'MC3' (Fig. 1). Nielsen and Schovsbo (2011, 2015) reconstructed the depositional environment of stratigraphic successions, reporting a gradient from proximal inner-shelf to mid-shelf and outer-shelf deposition below storm wave base. Inner-shelf deposition is recognised in all cores by abundant cross-bedding features within siltstones and generally coarser lithologies accompanying falling stage system tracts (FSSTs). Mid-shelf deposition is expressed as green silts and black shales with common glauconitic horizons and silty distal storm beds. Outer-shelf deposition is recognised by the presence of laminated mudstones and bioturbated siltstones in the absence of current features.

Results

Dominant water column redox conditions were determined *via* iron (Fe) speciation and trace metal systematics on mudstones and silts. Fe speciation relies on the quantification of highly reactive Fe (Fe_{HR}) relative to total Fe (Fe_T). Anoxic settings promote the formation of authigenic Fe minerals in the water column, resulting in Fe_{HR} enrichments in underlying sediments, with typically $Fe_{HR}/Fe_T \geq 0.38$ (Poulton and Canfield, 2011). By contrast, sediments deposited under oxic water columns lack Fe_{HR} enrichments, with $Fe_{HR}/Fe_T < 0.22$. Ratios between 0.22-0.38 are equivocal, and may represent either anoxic or oxic conditions, due to partial transformation of Fe_{HR} to sheet silicates during burial. We used Fe_T/Al enrichments (≥ 0.6) to evaluate this mechanism in instances of equivocal Fe_{HR}/Fe_T, since the ratio remains unaffected by diagenesis (Lyons and Severmann, 2006). For anoxic samples, ferruginous conditions are distinguished from euxinic settings by quantifying the extent of sulphidation of Fe_{HR}, whereby $Fe_P/Fe_{HR} \geq 0.7$ is characteristic of euxinic deposition and $Fe_P/Fe_{HR} < 0.7$ indicates ferruginous conditions (Poulton and Canfield, 2011).

Of the eight cores analysed, seven show marked stratigraphic shifts between oxic and anoxic deposition (Fig. 2). High concentrations of total organic carbon (TOC, up to ~20 %) are associated with anoxic conditions, reflecting enhanced organic carbon preservation and supply, with the latter exerting a primary control on the development of anoxia. LC1 records dominantly anoxic conditions at the base of
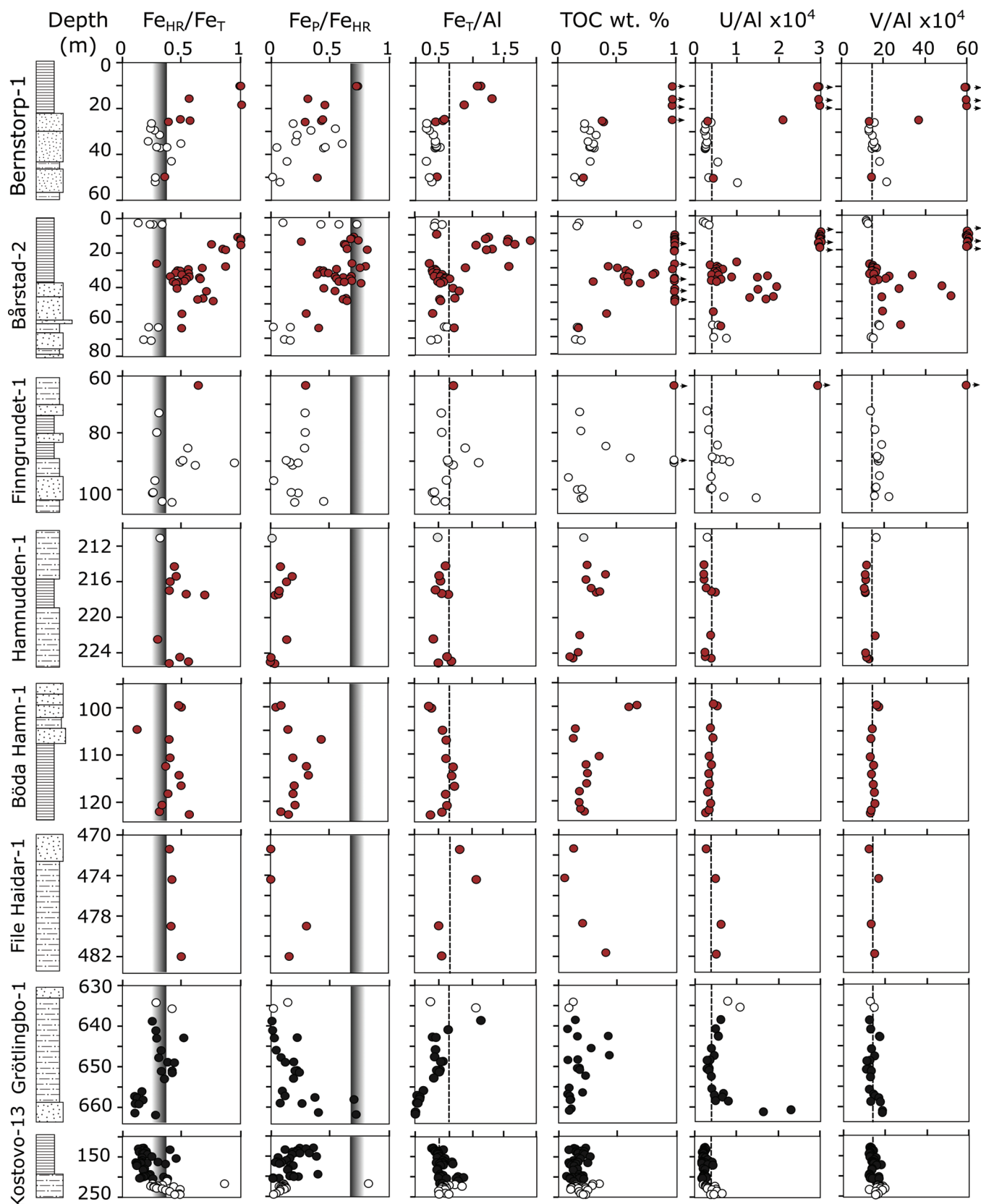
Figure 2   Geochemical data. Inner-, mid-, and outer-shelf environments are indicated by open, red and black symbols, respectively. Grey shadows delimit redox domains and dashed lines represent average shale values. Black arrows are for outpassing data points. Maximum values for U/Al and V/Al are 54 and 434 ppm/wt. %, respectively.

Kostovo-13, whereas oxic conditions prevail in the upper part of the core. Through LC2 and MC3, water column conditions are characterised predominantly by ferruginous anoxia, with some euxinic horizons towards the top of Bårstad-2 and Bernstorp-1. Within these latter strata, oxic conditions prevail at the base of Grötlingbo-1 and throughout all FSSTs (Figs. 1 and 2).

Redox variations between sequences are likely to reflect temporal changes. Furthermore, the core availability did not permit us to track each sequence in their full lateral expression. Therefore, in order to integrate water column redox data into a palaeo-environmental framework, we used the reconstructions of shelf environments in the Baltic Basin (Nielsen

and Schovsbo 2011, 2015) as binning discriminants (Fig. 3a). This statistical approach allows us to build a time-independent model for the redox architecture of the basin. Throughout the deposition of all successions, we observe statistically significant differences in the redox chemistry of inner-, mid- and outer-shelf environments (Table S-2). Oxic conditions systematically dominate throughout FSSTs, inner- and outer-shelf settings. Anoxic conditions, by contrast, tend to prevail in mid-shelf environments. Such distribution strongly suggests that the shelf was largely oxygenated at this time, with an expansion of anoxia limited to mid-shelves (Fig. 4). Trace metal (U and V) variations support Fe_T/Al and Fe speciation data, with pronounced sedimentary enrichments under euxinic water column conditions (Fig. 2). We note that for some instances of apparent oxic deposition based on Fe speciation (*e.g.*, at the basal and uppermost parts of the Grötlingbo-1 core), U enrichments are coeval with muted V enrichments, indicating low-oxygen conditions (Zhang *et al.*, 2016), comparable to that seen in modern OMZs (see Supplementary Information for details).

We complemented the inorganic redox proxies with biomarker indicators selected from mid-shelf sediments (Finngrundet-1, Bårstad-2, Bernstorp-1). The ratio of pristane to phytane (Pr/Ph) is low (0.46-0.79), supporting a dominantly anoxic mid-depth water column (Schwark and Frimmel, 2004). In these anoxic environments, 2,3,6-trimethyl aryl isoprenoids (AI) likely derived from anaerobic phototrophic green sulphur bacteria (GSB), and their detection indicates that the water column was temporarily anoxic up to the photic zone (Brocks *et al.*, 2005). The ratio between shorter- (C_{13} to C_{17}) and longer-chain (C_{18} to C_{22}) AI (the AI ratio, AIR) is used as a measure of oxidative degradation during deposition (Schwark and

Frimmel, 2004). Despite AI production in anoxic settings, the range and magnitude of AIR values (1.3 to 5.8) provide independent support for transient oxygenated conditions beneath the anoxic zone (Fig. 3b). Together with our Fe speciation data, this suggests that anoxic mid-depth waters overlaid oxygenated waters, enhancing oxidative degradation of AI during deposition.

Further evidence for distinct redox conditions across the shelf comes from the record of 'small carbonaceous fossils' (SCFs) (Butterfield and Harvey, 2012), found in oxic inner- and outer-shelf settings and ferruginous mid-shelf environments (Fig. 1). All recognisable SCFs are the remains of benthic aerobic animals, including *Wiwaxia*, stem-annelids, priapulids and palaeoscolecid worms (Fig. 3c). In contrast to sparsely fossiliferous mid-shelves, inner- and outer-shelf facies preserved most diverse SCFs assemblages, along with conspicuous burrows and bioturbation fabrics (Slater *et al.*, 2017). These palaeontological data corroborate the geochemical signatures for oxygenated inner- and outer-shelf environments (Fig. 3c). Fossilisation is of course a combination of both organismal ecology and taphonomic opportunity. Transient ferruginous conditions represent the dynamic interface between the oxic conditions where most metazoans live, and the anoxic conditions necessary to preserve non-biomineralising forms. Therefore, the apparently paradoxical persistence of SCFs in ferruginous settings may imply an iron shuttle from the core to the edges of the OMZ, enhancing the Fe_{HR} flux to oxygenated settings, or more likely dynamic oscillations between oxic and ferruginous water column conditions – in contrast to more permanently anoxic mid-shelves which were devoid of benthic metazoans and prone to euxinia.
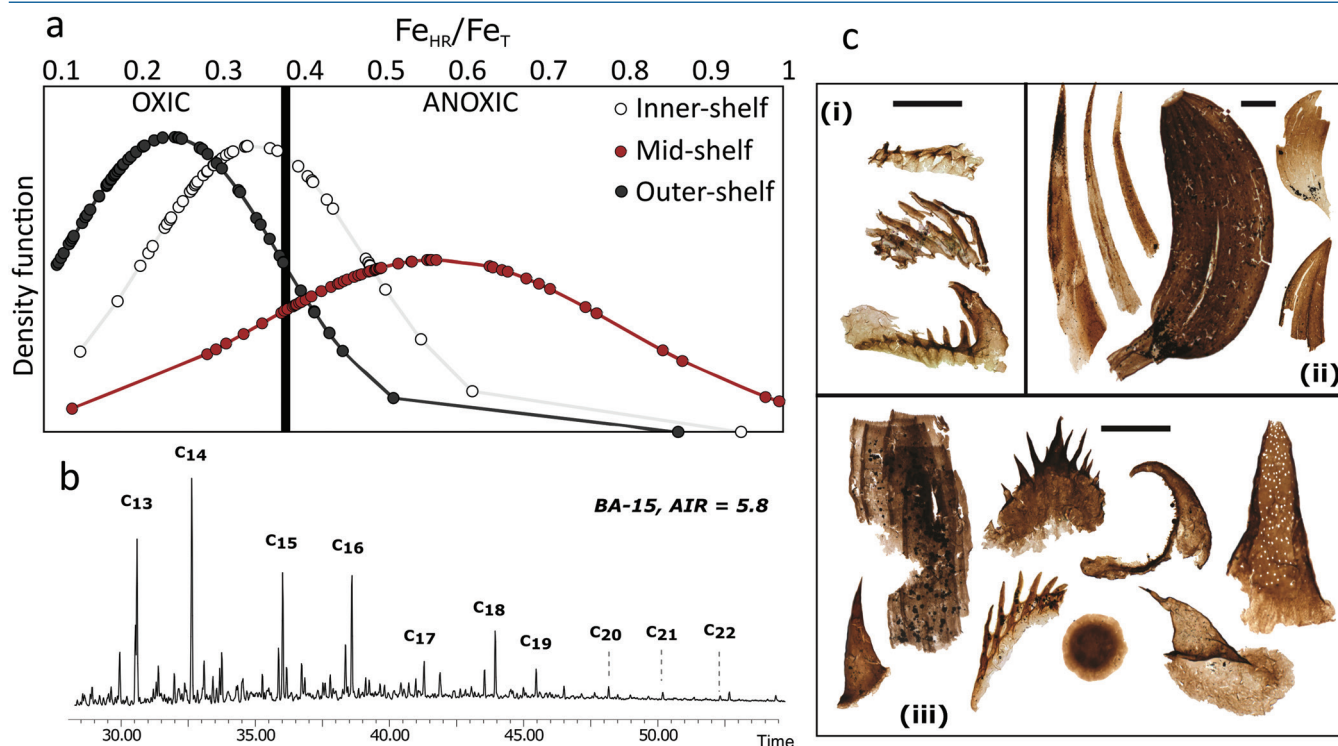

Figure 3   (a) Distribution of redox ratios (*n* = 183), binned as a function of their depositional environment. Inner- and outer-shelf environments show significantly more oxic redox populations than corresponding mid-shelves (*t* test *p* << 0.05). (b) Example of *m/z* = 134 partial ion chromatogram revealing the presence of 2,3,6 trimethyl aryl isoprenoids (AI) in mid-shelf facies. High ratios of short- to long-chain AI (AIR) point to strongly varying, intermittent oxygen exposure levels. (c) SCF assemblages from (i) inner-shelf (denticulate metazoan structures), (ii) mid-shelf (protoconodont spines alongside occasional *Wiwaxia* sclerites) and (iii) outer-shelf environments (priapulid, palaeoscolecid and annelid remains). Scale bars are 100 μm.
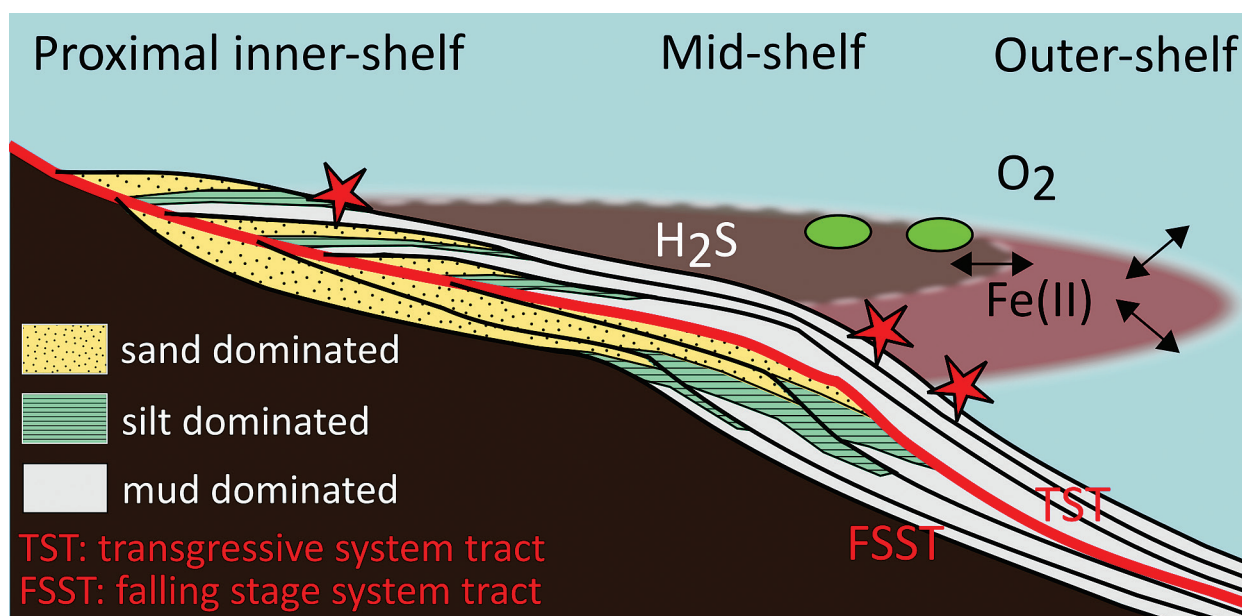
Figure 4 Redox architecture reconstruction, with oxic conditions above and below anoxic settings. Ferruginous conditions dominate in the OMZ, but euxinia develops in zones of increased organic carbon delivery. Metazoan body fossils recovery is shown by the red stars. Evidence for phototrophic GSB (green ovals) in mid-shelf settings corroborates geochemical and palaeontological redox indicators.

Implications

Our data provide evidence for a lateral expression of redox variation, which resembles the structure of modern OMZs (Fig. 4), although oxygen depletion was likely more pronounced and at shallower depths than in modern counterparts. Gentle topographical slope and reduced circulation in the relatively shallow Baltic Basin may have further exacerbated the role of benthic oxygen uptake, analogous to shallow OMZs (Brandt *et al.*, 2015). The discovery of OMZ denitrification in early Cambrian successions of China (Hammarlund *et al.*, 2017) suggests that our model may have been a common feature of contemporaneous margins. The record of ancient marine sedimentary rocks is certainly biased towards continental margins, which promotes the sampling of environments prone to host OMZs. Thus, in the absence of detailed spatial and temporal resolution, apparent horizontal stratification may often capture the upper boundary of OMZs, over-estimating global deep-water anoxia. By contrast, the recognition of such structure would explain the large discrepancies reported through the Neoproterozoic-Cambrian transition (*e.g.*, Sperling *et al.*, 2015b). Our data augments emerging views of early Cambrian expanded marine oxygenated conditions (Chen *et al.*, 2015; Li *et al.*, 2017), supporting the establishment of a modern-like ocean architecture during the 'explosion' of metazoan diversity (Butterfield, 2018).

Conclusion

Identification of dynamic wedge-shaped OMZs along the margins of the early Cambrian Baltic Basin raises the question of the antiquity of such structures. The evolutionary switch from a prokaryote- to eukaryote-dominated biological pump is thought to have played an essential role in the ventilation of the deep ocean (Butterfield, 2009, 2018; Lenton *et al.*, 2014). The subsequent establishment of modern-type OMZs, as identified in the early Cambrian ocean, may have developed as a consequence of contemporaneous metazoan expansion, whereby animal activity maintains high levels of oxygen depletion in OMZs (Bianchi *et al.*, 2013). However, OMZ structures may track back to older, Mesoproterozoic oceans (Zhang *et al.*,

2016). Although fundamental differences in pre-metazoan biological pump may have given terminal Proterozoic OMZs a distinct expression (presumably thicker and shallower), this overall geometry may have been a prevalent feature of late Precambrian oceans.

Author contributions

RG, BJS, THPH and NJB collected samples. RG extracted and interpreted geochemical data with significant contributions from BJN, JJB and SWP. BJS extracted and interpreted palaeontological data with significant contributions from THPH and NJB. RG and BJS wrote the manuscript, with significant contributions from all co-authors.

Additional Information

Supplementary Information accompanies this letter at http://www.geochemicalperspectivesletters.org/article1806.

source are credited. Additional information is available at http://www.geochemicalperspectivesletters.org/copyright-and-permissions.

Cite this letter as: Guilbaud, R., Slater, B.J., Poulton, S.W., Harvey, T.H.P., Brocks, J.J., Nettersheim, B.J., Butterfield, N.J. (2018) Oxygen minimum zones in the early Cambrian ocean. *Geochem. Persp. Let.* 6, 33-38.

References

BIANCHI, D., GALBRAITH, E.D., CAROZZA, D.A., MISLAN, K.A.S., STOCK, C.A. (2013) Intensification of open-ocean oxygen depletion by vertically migrating animals. *Nature Geoscience* 6, 545–548.

BRANDT, P., BANGE, H.W., BANYTE, D., DENGLER, M., DIDWISCHUS, S.-H., FISCHER, T., GREATBATCH, R.J., HAHN, J., KANZOW, T., KARSTENSEN, J., KÖRTZINGER, A., KRAHMANN, G., SCHMIDTKO, S., STRAMMA, L., TANHUA, T., VISBECK, M. (2015) On the role of circulation and mixing in the ventilation of oxygen minimum zones with a focus on the eastern tropical North Atlantic. *Biogeosciences (BG)* 12, 489–512.

BROCKS, J.J., LOVE, G.D., SUMMONS, R.E., KNOLL, A.H., LOGAN, G.A., BOWDEN, S.A. (2005) Biomarker evidence for green and purple sulphur bacteria in a stratified Palaeoproterozoic sea. *Nature* 437, 866–870.

BUTTERFIELD, N.J. (2009) Oxygen, animals and oceanic ventilation: an alternative view. *Geobiology* 7, 1–7.

BUTTERFIELD, N.J. (2018) Oxygen, animals and aquatic bioturbation: An updated account. *Geobiology* 16, 3–16.

BUTTERFIELD, N., HARVEY, T. (2012) Small carbonaceous fossils (SCFs): a new measure of early Paleozoic paleobiology. *Geology* 40, 71–74.

CANFIELD, D.E., POULTON, S.W., NARBONNE, G.M. (2007) Late-Neoproterozoic Deep-Ocean Oxygenation and the Rise of Animal Life. *Science* 315, 92–95.

CANFIELD, D.E., POULTON, S.W., KNOLL, A.H., NARBONNE, G.M., ROSS, G., GOLDBERG, T., STRAUSS, H. (2008) Ferruginous Conditions Dominated Later Neoproterozoic Deep-Water Chemistry. *Science* 321, 949–952.

CHEN, X., LING, H.-F., VANCE, D., SHIELDS-ZHOU, G.A., ZHU, M., POULTON, S.W., OCH, L.M., JIANG, S.-Y., LI, D., CREMONESE, L., ARCHER, C. (2015) Rise to modern levels of ocean oxygenation coincided with the Cambrian radiation of animals. *Nature Communications* 6, 7142.

GILL, B.C., LYONS, T.W., YOUNG, S.A., KUMP, L.R., KNOLL, A.H., SALTZMAN, M.R. (2011) Geochemical evidence for widespread euxinia in the Later Cambrian ocean. *Nature* 469, 80–83.

HAGENFELDT, S.E. (1994) The Cambrian File Haidar and Borgholm Formations in the central Baltic and south central Sweden. *Stockholm Contributions in Geology* 43, 69–110.

HAMMARLUND, E.U., GAINES, R.R., PROKOPENKO, M.G., QI, C., HOU, X.-G., CANFIELD, D.E. (2017) Early Cambrian oxygen minimum zone-like conditions at Chengjiang. *Earth and Planetary Science Letters* 475, 160–168.

JIN, C., LI, C., ALGEO, T.J., PLANAVSKY, N.J., CUI, H., YANG, X., ZHAO, Y., ZHANG, X., XIE, S. (2016) A highly redox-heterogeneous ocean in South China during the early Cambrian (~529–514 Ma): Implications for biota-environment co-evolution. *Earth and Planetary Science Letters* 441, 38–51.

LENTON, T.M., BOYLE, R.A., POULTON, S.W., SHIELDS-ZHOU, G.A., BUTTERFIELD, N.J. (2014) Co-evolution of eukaryotes and ocean oxygenation in the Neoproterozoic era. *Nature Geoscience* 7, 257–265.

LI, C., JIN, C., PLANAVSKY, N.J., ALGEO, T.J., CHENG, M., YANG, X., ZHAO, Y., XIE, S. (2017) Coupled oceanic oxygenation and metazoan diversification during the early–middle Cambrian? *Geology* 743–746.

LYONS, T.W., SEVERMANN, S. (2006) A critical look at iron paleoredox proxies: new insights from modern euxinic marine basins. *Geochimica et Cosmochimica Acta* 70, 5698–5722.

NIELSEN, A.T., SCHOVSBO, N.H. (2011) The Lower Cambrian of Scandinavia: depositional environment, sequence stratigraphy and palaeogeography. *Earth-Science Reviews* 107, 207–310.

NIELSEN, A.T., SCHOVSBO, N.H. (2015) The regressive Early-Mid Cambrian 'Hawke Bay Event' in Baltoscandia: Epeirogenic uplift in concert with eustasy. *Earth-Science Reviews* 151, 288–350.

PLANAVSKY, N.J., McGOLDRICK, P., SCOTT, C.T., LI, C., REINHARD, C.T., KELLY, A.E., CHU, X., BEKKER, A., LOVE, G.D., LYONS, T.W. (2011) Widespread iron-rich conditions in the mid-Proterozoic ocean. *Nature* 477, 448–451.

POULTON, S.W., CANFIELD, D.E. (2011) Ferruginous Conditions: A Dominant Feature of the Ocean through Earth's History. *Elements* 7, 107–112.

POULTON, S.W., FRALICK, P.W., CANFIELD, D.E. (2010) Spatial variability in oceanic redox structure 1.8 billion years ago. *Nature Geoscience* 3, 486–490.

SCHWARK, L., FRIMMEL, A. (2004) Chemostratigraphy of the Posidonia Black Shale, SW-Germany: II. Assessment of extent and persistence of photic-zone anoxia using aryl isoprenoid distributions. *Chemical Geology* 206, 231–248.

SLATER, B.J., HARVEY, T.H.P., GUILBAUD, R., BUTTERFIELD, N.J. (2017) A cryptic record of Burgess Shale-type diversity in the early Cambrian of Baltica. *Palaeontology* 60, 117–140.

SPERLING, E.A., KNOLL, A.H., GIRGUIS, P.R. (2015a) The Ecological Physiology of Earth's Second Oxygen Revolution. *Annual Review of Ecology, Evolution, and Systematics* 46, 215–235.

SPERLING, E.A., WOLOCK, C.J., MORGAN, A.S., GILL, B.C., KUNZMANN, M., HALVERSON, G.P., MACDONALD, F.A., KNOLL, A.H., JOHNSTON, D.T. (2015b) Statistical analysis of iron geochemical data suggests limited late Proterozoic oxygenation. *Nature* 523, 451–454.

TOSTEVIN, R., WOOD, R.A., SHIELDS, G.A., POULTON, S.W., GUILBAUD, R., BOWYER, F., PENNY, A.M., HE, T., CURTIS, A., HOFFMANN, K.H., CLARKSON, M.O. (2016) Low-oxygen waters limited habitable space for early animals. *Nature Communications* 7, 12818.

VON STRANDMANN, P.A.P., STÜEKEN, E.E., ELLIOTT, T., POULTON, S.W., DEHLER, C.M., CANFIELD, D.E., CATLING, D.C. (2015) Selenium isotope evidence for progressive oxidation of the Neoproterozoic biosphere. *Nature Communications* 6, 10157.

WOOD, R.A., POULTON, S.W., PRAVE, A.R., HOFFMANN, K.-H., CLARKSON, M.O., GUILBAUD, R., LYNE, J.W., TOSTEVIN, R., BOWYER, F., PENNY, A.M., CURTIS, A., KASEMANN, S.A. (2015) Dynamic redox conditions control late Ediacaran metazoan ecosystems in the Nama Group, Namibia. *Precambrian Research* 261, 252–271.

ZHANG, S., WANG, X., WANG, H., BJERRUM, C.J., HAMMARLUND, E.U., COSTA, M.M., CONNELLY, J.N., ZHANG, B., SU, J., CANFIELD, D.E. (2016) Sufficient oxygen for animal respiration 1,400 million years ago. *Proceedings of the National Academy of Sciences* 113, 1731–1736.